Diagn Interv Radiol 2018; 24:195–202

CHEST IMAGING

ORIGINAL ARTICLE

Dynamic contrast-enhanced MRI for advanced esophageal cancer response assessment after concurrent chemoradiotherapy

Na-Na Sun
Chang Liu
Xiao-Lin Ge
Jie Wang

PURPOSE
We aimed to evaluate the treatment response of patients with esophageal cancer after concurrent chemoradiation therapy (CRT) using dynamic contrast-enhanced magnetic resonance imaging (DCE-MRI).

METHODS
This retrospective study included 59 patients with histologically confirmed esophageal squamous cell carcinoma. The patients underwent DCE-MRI before and 4 weeks after CRT. Patients with complete response were defined as the CR group; partial response, stable disease, and progressive disease patients were defined as the non-CR group. DCE-MRI parameters (K^{trans}, V_e, and K_{ep}) were measured and compared between pre- and post-CRT in the CR and non-CR groups, respectively. Pre-CRT and post-CRT parameters were used to calculate the absolute change and the ratio of change. DCE-MRI parameters were compared between the CR and non-CR groups. Receiver operating characteristic (ROC) curves were used to verify diagnostic performance.

RESULTS
Patients with higher T-stage esophageal cancer might present with poorer response. After CRT, the K^{trans} and K_{ep} values significantly decreased in the CR group, whereas only K_{ep} value decreased in the non-CR group. The post-K^{trans} and post-K_{ep} values were observed to be significantly lower in the CR group than in the non-CR group. The absolute change and ratio of change of both K^{trans} and K_{ep} were higher in the CR group than in the non-CR group. Based on ROC analysis, the ratio of change in K^{trans} was the best parameter to assess treatment response (AUC= 0.840).

CONCLUSION
DCE-MRI parameters are valuable in predicting and assessing concurrent CRT response for advanced esophageal cancer.

Esophageal cancer is the fourth most common cancer in China with five-year survival rates ranging from 15% to 40% (1–3). Patients with early-stage esophageal cancer are usually treated with endoscopic submucosal dissection (ESD) or esophagectomy. However, for patients with unresectable advanced esophageal cancer or who cannot tolerate esophagectomy, chemoradiation therapy (CRT) is a priority. CRT prolonged lifetime of many patients with esophageal cancer, but some patients cannot benefit from it, which depends on the patients' response (4). Meanwhile, side effects caused by CRT including bone marrow suppression, esophagitis, pericarditis, and pneumonia should not be overlooked (3). Thus, useful methods are required to assess and predict the response to CRT.

Conventional imaging modalities, including X-ray, computed tomography (CT) and magnetic resonance imaging (MRI), have been used to assess CRT response for esophageal cancer. These imaging modalities focus on the morphologic changes of esophageal mucosa, tumor size, and enhancement. Positron emission tomography-computed tomography is valuable to assess the volumetric change and metabolic status of tumor. Published studies have demonstrated that functional MRI can be employed as a potential method for monitoring and predicting treatment response in esophageal cancer (5–14). Functional imaging by dynamic contrast-enhanced MRI (DCE-MRI) has been investigated in recent years to assess vascular permeability. Previous studies have investigated the

From the Departments of Radiology (N-N.S., C.L.) and Radiotherapy (X-L.G., J.W. ✉ *wangjie2118@126.com*), The First Affiliated Hospital of Nanjing Medical University, Nanjing, China.

Received 10 October 2017; revision requested 29 October 2017; last revision received 27 February 2018; accepted 12 March 2018.

DOI 10.5152/dir.2018.17369

You may cite this article as: Sun N-N, Liu C, Ge X-L, Wang J. Dynamic contrast-enhanced MRI for advanced esophageal cancer response assessment after concurrent chemoradiotherapy. Diagn Interv Radiol 2018; 24:195–202.

potential role of DCE-MRI in evaluating treatment response in head, neck, breast, oral, cervical, rectal cancers, and soft tissue sarcoma (7–14). Some studies have reported the value of DCE-MRI using pharmacokinetic parameters in patients with esophageal cancer (4, 14–16). In the literature, DCE-MRI has been used in esophageal cancer to differentiate between adenocarcinoma and squamous cell carcinoma (15), assess chemotherapy response (14), and distinguish adenocarcinoma from normal esophageal wall (16).

In this study, we aimed to investigate the performance of DCE-MRI parameters in assessing and predicting treatment response after CRT in patients with advanced esophageal cancer. We focused on evaluating treatment response between pre-CRT and post-CRT and compared complete responders and non-complete responders in a larger sample size than previously reported (14); in addition, we analyzed the changes in absolute values and and ratios of DCE-MRI parameters.

Methods

Patients

This retrospective study was approved by the institutional review board of our hospital and the requirement for written informed consent was waived due to the retrospective nature of the study. From September 2014 to December 2016, patients who had undergone esophageal DCE-MRI scanning were screened. Inclusion criteria were: pathologically confirmed advanced esophageal squamous cancer by esophagoscopy; 3.0 T DCE-MRI scanning prior to concurrent CRT (pre-CRT); 3.0 T DCE-MRI 4 weeks after CRT (post-CRT); and adequate MRI quality for analysis.

From September 2014 to December 2016, 112 patients with suspicious esophageal lesions underwent DCE-MRI. The following patients were excluded: 18 patients with T1-stage esophageal cancer or high-grade intraepithelial neoplasia, 8 patients with leiomyoma, 23 patients without pre-CRT or post-CRT MRI examinations, and 4 patients with poor image artifacts. Finally, 59 patients were included in this retrospective study (Table 1). According to Revised Response Evaluation Criteria in Solid Tumors (RECIST) Guideline version 1.1 (17), there were 38 patients with complete response, 9 patients with partial response, 8 patients with stable disease, and 4 patients with progressive disease. For the purpose of analysis, patients were grouped as complete response (CR) group (n=38) and non-complete response (non-CR) group (n=21).

Main points

- We investigated the role of quantitative DCE-MRI parameters to assess and predict chemoradiotherapy (CRT) response for patients with advanced esophageal cancer.
- Patients with high T-stage esophageal cancer may present with poor CRT response.
- The MRI parameter pre-K^{trans} is valuable in predicting treatment response to CRT.
- Marked reductions in K^{trans} and K_{ep} values were associated with good CRT response.
- ROC curves of diagnostic performance of $r\Delta K^{trans}$ showed substantial advantage for assessing treatment response to CRT.

Chemoradiotherapy

Radiation therapy at a dose of 60 Gy (2Gy/fraction, 5 fractions/week) was delivered to primary tumor site and involved lymph nodes. Chemotherapy was performed concurrently with radiation therapy by using liposomal paclitaxel 35 mg/m^2 plus cisplatin 25 mg/m^2 administered on day 1 weekly for 6 weeks.

MRI protocols

MRI examinations were performed on a 3.0 Tesla MRI scanner (MAGNETOM Trio-Tim; Siemens) with a 16-channel torso coil. The MRI sequences included: transverse T1-weighted imaging, transverse and sagittal T2-weighted imaging, and transverse DCE-MRI. DCE-MRI scanning included two parts: before contrast injection, transverse volume interpolated breath-hold examination (VIBE) sequences were scanned with three flip angles (α= 5°,10°,15°) to calculate T1 mapping; then, DCE images were acquired with VIBE sequence (repetition time, 5.22 ms; echo time, 1.81 ms; field of view, 21×28 cm^2; matrix, 256×138; slice thickness, 3 mm; number of phases, 32; temporal resolution, 7s). A bolus of MRI contrast (Gadodiamide, Omniscan, GE HealthCare) was injected at a rate of 2.5 mL/s through a 20-gauge antecubital intravenous line at the third phase of DCE scanning. Bolus injection was performed with a MRI-compatible power injector (Spectris; Stellant MR Injection System) followed by 15 mL saline flush.

DCE-MRI analysis

Two digestive radiologists with 5 and 9 years of experience, respectively, studied the parameters on successive magnetic resonance images in consensus. All DCE-MRI data were transferred in Digital Imaging and Communications in Medicine (DICOM) format and processed with OmniKinetics software (GE Healthcare) by extended Tofts Liner model. Individual based arterial input function (AIF) was picked for each case because it varies between individuals in reflection of cardiac output, vascular tone and renal function. Referring to T2-weighted imaging and contrast-enhanced T1-weighted imaging, all regions of interest (ROIs) of esophageal cancer were manually set, encompassing the entire tumor area but excluding necrosis, peripheral fat, and blood vessels. The heart motion might lead to unclear tumor border. Thus, when we drew the ROI of the tumor, we made the ROI slightly smaller in size than observed tumor size to reduce the influence of partial volume effect. Three quantitative parameters obtained from DCE-MRI: K^{trans} (min^{-1}), transfer constant; K_{ep} (min^{-1}), efflux rate constant; and V_e, ratio of extracellular-extravascular space volume to tissue volume.

Statistical analysis

All statistical analyses were performed using SPSS 21.0 statistical software (IBM Corp.). The Kolmogorov-Smirnov's test was used to determine whether the quantitative parameters are subjected to normal distribution. Normally distributed data were presented as means ± standard deviation; not normally distributed data were presented by median and range. Categorical data (including gender, location, clinical T-stage and N-stage) were presented as count and frequency and compared by chi-square test. Fisher's exact test was used when chi-square conditions were not met. Numerical normally distributed data were compared with two independent sample t test; Mann-Whitney U test was used for comparison of not normally distributed data. Paired Student's t test was used to identify significant differences of the parameters between pre-CRT and post- CRT in both CR and non-CR groups. Absolute value of change and ratio of change were calculated as follows: Change in K^{trans} (ΔK^{trans} = post-CRT K^{trans} value – pre-CRT K^{trans} value); change ratio of K^{trans} ($r\Delta K^{trans}$ = ΔK^{trans} /pre-CRT K^{trans} value). The same calculation method was applied to the other two parameters

(K_{ep} and V_e). Independent sample t test was used to identify significant differences of the parameters between the CR and non-CR groups. Receiver operating characteristic (ROC) analyses were performed to find a reasonable threshold to differentiate CRT good responders from poor responders. The optimal thresholds were obtained by calculating the maximal Youden index (Youden index = sensitivity + specificity-1). Meanwhile, the areas under the curve (AUCs) were compared using nonparametric methods for comparison of ROC curves. Comparisons were considered statistically significant for $P < 0.05$.

Results

The demographic data of all patients are summarized in Table 1. There were 26 males (mean age, 61.8±10.1 years) and 12 females (mean age, 65.9±6.7 years) in the CR group, 16 males (mean age, 67.5±8.6 years) and 5 females (mean age, 65.4±6.0 years) in the non-CR group. No statistically significant difference was identified in gender, age, and location of esophageal cancer between the CR and non-CR groups. There was significant difference in clinical T-stage (P = 0.032) between the CR and non-CR groups, while no difference was observed in clinical N-stage (P = 0.212).

Comparisons of DCE-MRI parameters between pre-CRT and post-CRT are shown in Table 2. Both K^{trans} and K_{ep} significantly decreased from pre-CRT to post-CRT in the CR group ($P < 0.001$). The K_{ep} value also showed a marked reduction in the non-CR group (P = 0.028). K^{trans} also decreased in the non-CR group, but it did not approach statistical significance (P = 0.199). Although V_e values increased after CRT in both groups, the differences were not significant. Representative cases of the CR and non-CR groups are presented in Figs. 1 and 2, respectively. On pseudocolor images, warm colors imply a higher value of the parameter, while cool colors imply lower values.

Table 3 shows comparisons of DCE-MRI parameters between the CR and non-CR groups in unpaired analysis. In pre-CRT measurements, the K^{trans} values of the CR group were significantly higher than that of the non-CR group (P = 0.047). In assessment of treatment response to CRT, post-K^{trans} and post-K_{ep} values were significantly lower in the CR group than in the non-CR group (P = 0.002, $P < 0.001$). The changes in value and ratios of K^{trans} (ΔK^{trans}, $r\Delta K^{trans}$) and K_{ep} (ΔK_{ep}, $r\Delta K_{ep}$) showed significant difference between the CR and non-CR groups. From pre-CRT to post-CRT, the K^{trans} values showed tendency to decrease in both CR and non-CR groups (35% and 2.7% reduction, respectively). The K_{ep} values showed 41.6% decrease in the CR group and 6.4% in the non-CR group. The post-V_e values were lower when compared with pre-V_e in both groups, without reaching statistical significance. The performance of K^{trans}, K_{ep} and V_e parameters in predicting treatment response were assessed by ROC curve analysis (Table 4). In comparison with the other pre-CRT parameters, pre-K^{trans} values indicated good diagnostic performance (AUC=0.678). For post-CRT measurements, post-K_{ep} showed the highest AUC of 0.817, with a cutoff value of 1.031, sensitivity of 94.7%, and specificity of 57.1%. In terms of change, the AUC of ΔK^{trans} was highest

Table 1. Summary of demographic data in 59 patients

	CR group (n=38)	non-CR group (n=21)	*P*
Gender			0.528
Men	26 (68.4)	16 (76.2)	
Women	12 (31.6)	5 (23.8)	
Mean age (years)			
All patients	63.3±9.3	67.1±8.1	0.542
Men	61.8±10.1	67.5±8.6	0.416
Women	65.9±6.7	65.4±6.0	0.685
Clinical T-stage			0.032*
II	13 (34.2)	1 (4.8)	
III	16 (42.1)	11 (52.4)	
IV	9 (23.7)	9 (42.9)	
Clinical N-stage			0.212
N0	12 (31.6)	4 (19.0)	
N1	10 (26.3)	7 (33.3)	
N2	9 (23.7)	9 (42.9)	
N3	7 (18.4)	1 (4.8)	
Location			0.087
Cervical	3 (7.9)	2 (9.5)	
Upper thoracic	16 (42.1)	3 (14.3)	
Middle thoracic	15 (39.5)	10 (47.6)	
Distal	4 (10.5)	6 (28.6)	

Data are presented as n (%).
CR, complete response; non-CR, non-complete response (partial response, stable disease, or progressive disease).
*$P < 0.05$.

Table 2. Comparison of DCE-MRI parameters between pre-CRT and post-CRT

	CR group			non-CR group		
	pre-CRT	post-CRT	*P*	pre-CRT	post-CRT	*P*
K^{trans}	0.576±0.132	0.363±0.100	<0.001	0.489±0.162	0.459±0.127	0.219
K_{ep}	1.431±0.466	0.762±0.204	<0.001	1.294±0.528	1.061±0.263	0.028
V_e	0.451±0.189	0.490±0.118	0.248	0.445±0.199	0.458±0.173	0.783

DCE-MRI, dynamic contrast-enhanced magnetic resonance imaging; CR, complete response; non-CR, non-complete response (partial response, stable disease, or progressive disease); CRT, chemoradiation therapy; K^{trans}, volume transfer constant between extravascular-extracellular space and blood plasma; K_{ep}, rate constant from extravascular extracellular space to blood plasma; V_e, extravascular-extracellular space volume per unit tissue volume.
The unit for K^{trans} and K_{ep} value is min^{-1}.

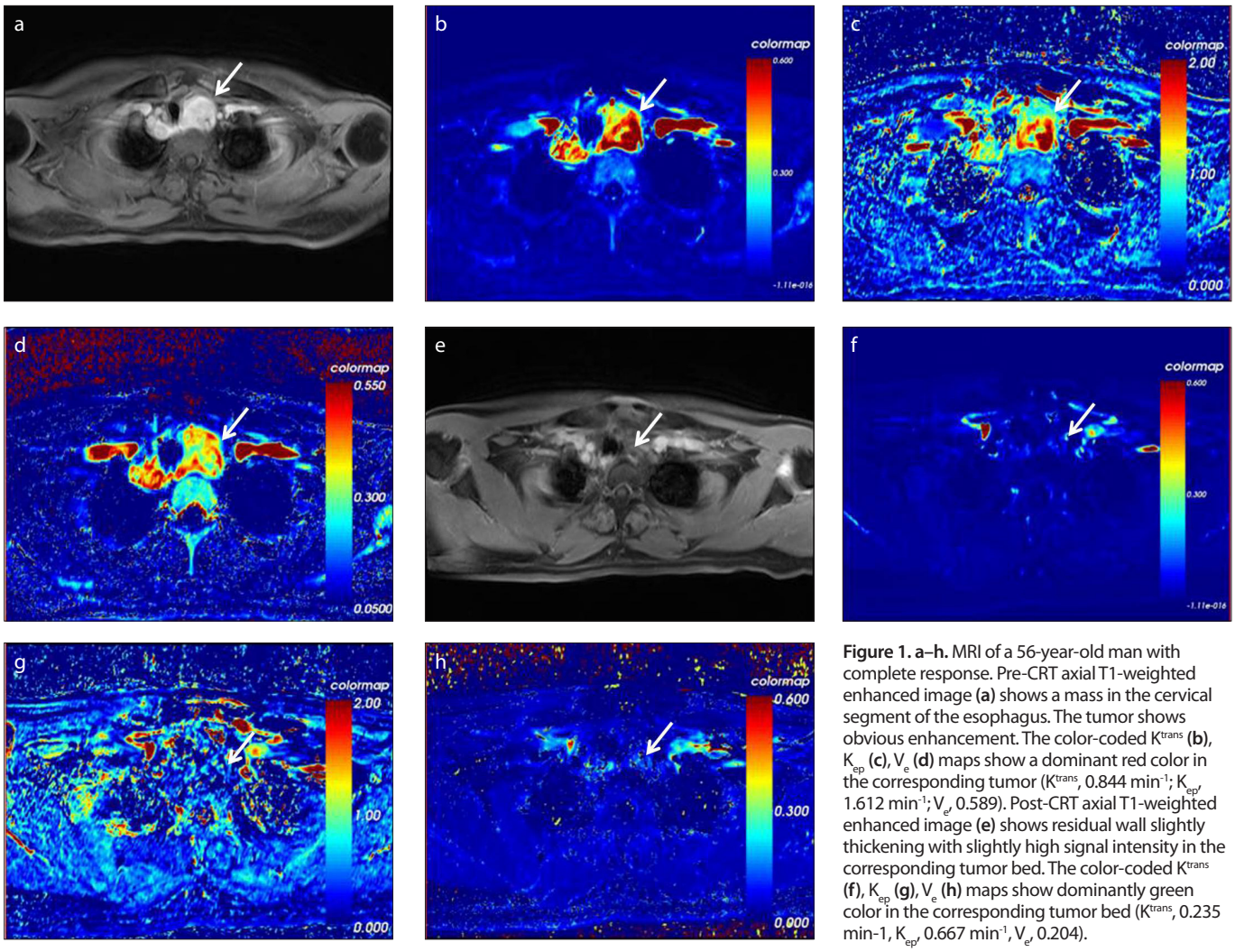

Figure 1. a–h. MRI of a 56-year-old man with complete response. Pre-CRT axial T1-weighted enhanced image **(a)** shows a mass in the cervical segment of the esophagus. The tumor shows obvious enhancement. The color-coded K^{trans} **(b)**, K_{ep} **(c)**, V_e **(d)** maps show a dominant red color in the corresponding tumor (K^{trans}, 0.844 min^{-1}; K_{ep}, 1.612 min^{-1}; V_e, 0.589). Post-CRT axial T1-weighted enhanced image **(e)** shows residual wall slightly thickening with slightly high signal intensity in the corresponding tumor bed. The color-coded K^{trans} **(f)**, K_{ep} **(g)**, V_e **(h)** maps show dominantly green color in the corresponding tumor bed (K^{trans}, 0.235 min-1, K_{ep}, 0.667 min^{-1}, V_e, 0.204).

at 0.816, with an optimal cutoff value of -0.206, sensitivity of 52.6%, and specificity of 95.2%. In terms of ratio of change, $r\Delta K^{trans}$ resulted in the highest AUC of 0.840, with the optimal cutoff value of -0.144, sensitivity of 89.5%, and specificity of 61.9%. ROC curves of diagnostic performance of the parameters for detecting CRT response were shown in Fig. 3.

Discussion

DCE-MRI is a widely used imaging method reflecting vascular perfusion and endothelial permeability of tumor microcirculation, which are regarded as the most important factors in assessment of CRT response. This study investigated the role of quantitative DCE-MRI parameters of pre- and post-CRT to assess and predict treatment response for patients with advanced esophageal cancer.

Our data showed that there was significant difference in clinical T-stage between the CR and non-CR groups, while no changes were observed in clinical N-stage, gender, age, and location of tumor. The percentage of clinical T2 stage patients in the non-CR group was lower than that in the CR group, suggesting that patients with higher T-stage esophageal cancer might have a poorer CRT response. Consistent with studies on oral cancer and esophageal cancer, our results also demonstrated that an advanced T-stage indicated a poor clinical response (10, 16).

The K^{trans} and K_{ep} values are closely associated with the degree of tumor microcirculation and angiogenesis. Compared with normal blood vessels, tumor neovascularization leads to increased permeability and perfusion, which means higher K^{trans} and K_{ep} values. Before CRT, the K^{trans} value was significantly higher in the CR group than in the non-CR group. Therefore, we assume that high pre-K^{trans} value is associated with good response. Our finding is in agreement with a recent study in patients with esophageal cancer that has also shown better treatment response with higher pre-CRT K^{trans} values (14). Other studies have also suggested that tumors with high K^{trans} values may have better treatment response compared with those with low K^{trans} values, because of better delivery of the chemotherapeutic agents and greater radiosensitivity (18–21). However, previous DCE-MRI studies were unable to show any correlation between pretreatment K^{trans} values and treatment response for oral cancer and rectal cancer (10, 18). We postulate that lower K^{trans} value in the non-CR group may indicate relatively lower blood perfusion which reduces the effectiveness of chemoradiation. Our observation is in accordance with previous investigations (18, 22–24). Among pre-CRT parameters, pre-K^{trans} values showed the highest AUC in predicting treatment response, suggesting that it can be a promising MRI biomarker.

We also found that the K^{trans} value in the CR group showed a significant decrease after CRT, a finding that corresponded well

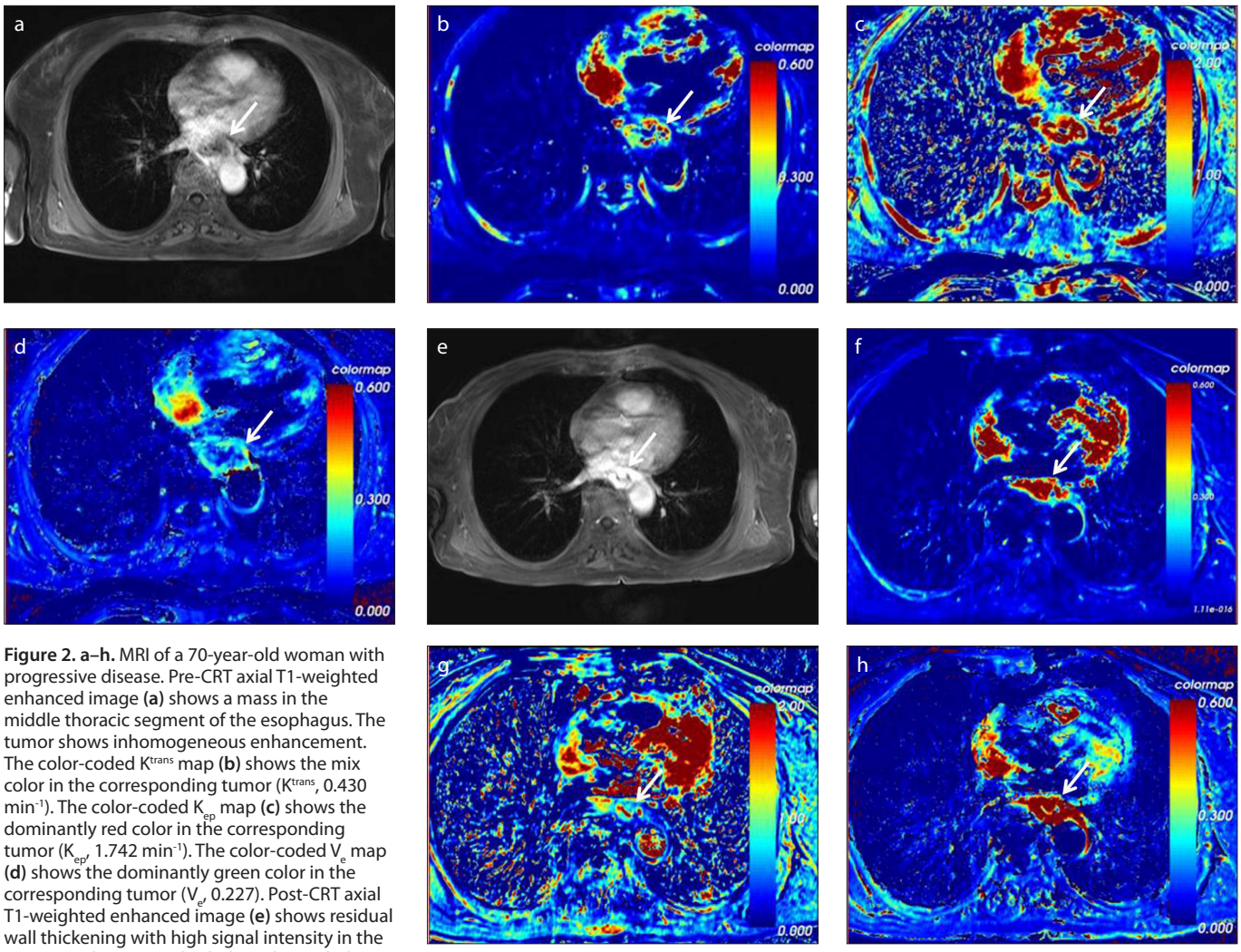

Figure 2. a–h. MRI of a 70-year-old woman with progressive disease. Pre-CRT axial T1-weighted enhanced image **(a)** shows a mass in the middle thoracic segment of the esophagus. The tumor shows inhomogeneous enhancement. The color-coded K^{trans} map **(b)** shows the mix color in the corresponding tumor (K^{trans}, 0.430 min^{-1}). The color-coded K_{ep} map **(c)** shows the dominantly red color in the corresponding tumor (K_{ep}, 1.742 min^{-1}). The color-coded V_e map **(d)** shows the dominantly green color in the corresponding tumor (V_e, 0.227). Post-CRT axial T1-weighted enhanced image **(e)** shows residual wall thickening with high signal intensity in the corresponding tumor bed. The color-coded K^{trans} map **(f)** shows increased red color in the corresponding tumor bed (K^{trans}, 0.598 min^{-1}). The color-coded K_{ep} map **(g)** shows mix color in the corresponding tumor bed (K_{ep}, 1.129 min^{-1}). The color-coded V_e map **(h)** shows increased red color in the corresponding tumor bed (V_e, 0.654).

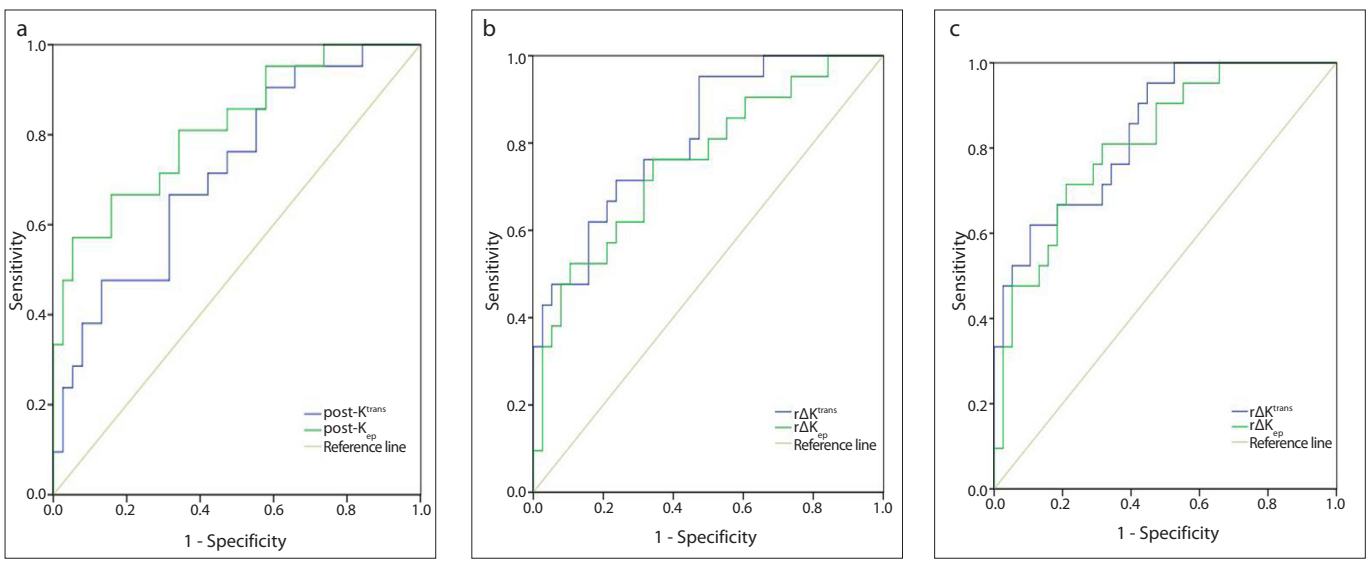

Figure 3. a–c. ROC curves of post-K^{trans} and post-K_{ep} **(a)**, ΔK^{trans} and ΔK_{ep} **(b)**, $r\Delta K^{trans}$ and $r\Delta K_{ep}$ **(c)** in assessing good treatment responders (post-K^{trans}, AUC=0.719; post-K_{ep}, AUC=0.817; ΔK^{trans}, AUC=0.816; ΔK_{ep}, AUC=0.757); $r\Delta K^{trans}$, AUC=0.840; $r\Delta K_{ep}$, AUC=0.813).

with those of previous studies (10, 22, 25). Kim et al. (22) attributed the contrasting changes and ratios of K^{trans} after CRT to a larger fibrotic area in good responders, but a substantial, residual, viable tumor area in poor responders. Other studies explained the decrease of K^{trans} value by lower microvessel density after CRT (23–26). This opinion also explains the increase in V_e value after CRT, although change and ratio of V_e value showed no statistical difference between pre- and post- CRT in this study. Our findings bear some similarities to the findings in a recent study, which revealed that higher K^{trans} values before therapy, lower K^{trans} values after therapy, and a large reduction in relative K^{trans} indicate good response (10, 18, 20, 22). The absolute $r\Delta K^{trans}$ of good responders in previous studies are divergent, ranging from 8.6% to 38.4% (10, 18, 20, 22). The present study revealed that the K_{ep} values representing vessel permeability decreased after CRT in both groups. Among post-CRT measurements, the post-K_{ep} value resulted in better diagnostic performance in assessing treatment response (AUC=0.817). Meanwhile, the absolute ΔK_{ep} and $r\Delta K_{ep}$ values in the CR group were significantly higher than those in the non-CR group. These findings are supported by previous studies in which the range of absolute $r\Delta K_{ep}$ was 20.3%–37.3% (10, 20, 27, 28). However, our study is inconsistent with a previous evaluation of treatment response in 25 patients with esophageal cancer (14). We speculate that these diverse results may be associated with the sample size and tumor heterogeneity. Thus, a larger sample size is needed to verify the results, and further investigation is warranted to determine whether tumor heterogeneity affects the quantitative parameters of DCE-MRI.

Previous studies reported that CRT could cause a significant increase in the V_e value

Table 3. Comparison of DCE-MRI parameters between the CR and non-CR groups

Parameters	CR group (n=3) mean±SD	non-CR group (n=21) mean±SD	*P*
Pre-K^{trans}	0.576±0.132	0.489±0.162	0.047
Post-K^{trans}	0.363±0.100	0.459±0.127	0.002*
ΔK^{trans}	-0.213±0.134	-0.040±0.137	<0.001*
$r\Delta K^{trans}$	-0.350±0.177	-0.027±0.334	<0.001*
Pre-K_{ep}	1.431±0.466	1.294±0.528	0.308
Post-K_{ep}	0.762±0.204	1.061±0.263	<0.001*
ΔK_{ep}	-0.668±0.446	-0.232±0.451	0.001*
$r\Delta K_{ep}$	-0.416±0.229	-0.064±0.376	<0.001*
Pre-V_e	0.451±0.189	0.445±0.199	0.903
Post-V_e	0.490±0.118	0.458±0.173	0.414
ΔV_e	0.028±0.202	0.014±0.223	0.793
$r\Delta V_e$	0.234±0.563	0.198±0.653	0.823

The unit for K^{trans} and K_{ep} value is $\times 10^{-3}$ mm^2/s.
CRT, chemoradiation therapy; K^{trans}, volume transfer constant between extravascular-extracellular space and blood plasma; K_{ep}, rate constant from extravascular extracellular space to blood plasma; V_e extravascular-extracellular space volume per unit tissue volume; ΔX, change in X; rΔX, change ratio of X.
*$P < 0.05$.

Table 4. Diagnostic performance of the parameters for the detection of response to CRT

Parameter	AUC	Sensitivity (%)	Specificity (%)	Cutoff value	Maximal Youden index	*P*
Pre-K^{trans}	0.678 (0.544–0.794)	68.4 (51.3–82.5)	66.7 (43.0–85.4)	0.509	35.1	0.011
Post-K^{trans}	0.719 (0.587–0.828)	68.4 (51.3–82.5)	66.7 (43.0–85.4)	0.403	35.1	0.003
ΔK^{trans}	0.816 (0.693–0.905)	52.6 (35.8–69.0)	95.2 (76.1–99.2)	-0.206	47.8	<0.001
$r\Delta K^{trans}$	0.840 (0.721–0.922)	89.5 (75.2–97.0)	61.9 (38.5–81.8)	-0.144	51.4	<0.001
Pre-K_{ep}	0.578 (0.442–0.705)	63.2 (46.0–78.2)	61.9 (38.5–81.8)	1.339	25.1	0.312
Post-K_{ep}	0.817 (0.695–0.906)	94.7 (82.2–99.2)	57.1 (34.0–78.1)	1.031	51.8	<0.001
ΔK_{ep}	0.757 (0.628–0.859)	65.8 (48.6–80.4)	76.2 (52.8–91.7)	-0.511	42.0	<0.001
$r\Delta K_{ep}$	0.813 (0.690–0.903)	78.9 (62.7–90.4)	71.4 (47.8–88.6)	-0.272	50.3	<0.001
Pre-V_e	0.546 (0.411–0.676)	81.6 (65.7–92.2)	47.6 (25.7–70.2)	0.349	29.2	0.553
Post-V_e	0.595 (0.459–0.721)	92.1 (78.6–98.2)	38.1 (18.2–61.5)	0.364	30.2	0.213
ΔV_e	0.563 (0.428–0.692)	68.4 (51.3–82.5)	52.4 (29.8–74.3)	-0.008	20.8	0.414
$r\Delta V_e$	0.566 (0.431–0.695)	68.4 (51.3–82.5)	52.4 (29.8–74.3)	-0.024	20.8	0.390

Data in parentheses indicate 95% confidence intervals.
CRT, chemoradiation therapy; AUC, area under the ROC curve; K^{trans}, volume transfer constant between extravascular-extracellular space and blood plasma; K_{ep}, rate constant from extravascular extracellular space to blood plasma; V_e, extravascular-extracellular space volume per unit tissue volume; ΔX, change in X; rΔX, change ratio of X.

which was associated with a better response (12, 14). A study assessing chemotherapy response in patients with osteosarcoma revealed that V_e might serve as a prognostic biomarker (29). Whereas, our data revealed no significant change in V_e values from pre- to post-CRT in the CR and non-CR groups. Other investigators also failed to find significant differences in the V_e value between the good and poor responders (18, 22). The findings might be attributed to the effectiveness of CRT in inhibiting the generation of tumor cells, leading to increase in the extravascular extracellular space (EES) and the volumetric proportion of the EES (14). The V_e value represents the motion space of water molecules, and is affected by blood flow. Increased blood flow can increase the contrast agent getting into the EES, so V_e cannot be used alone to evaluate the blood perfusion and EES. V_e is a comprehensive factor, which means that it is not definite in the evaluation of tumor angiogenesis.

Our study suffers from some limitations. First, the sample size in this present study might affect the accuracy of the results. Therefore, we need a larger sample size in further studies. Second, we did not compare DCE-MRI parameters with data from diffusion-weighted imaging (DWI). Past findings suggested that DWI could potentially provide complementary information about treatment response assessment and prediction (30, 31). Further study of the correlation analysis of DWI and DCE-MRI would be necessary for esophageal carcinoma. Finally, we did not investigate tumor heterogeneity. The diverse results in previous studies may be associated with tumor heterogeneity. Histogram analysis of DCE-MRI parameters might provide quantitative information about tumor heterogeneity.

Reportedly, some immunohistochemical, blood-based, mRNA-based, and gene expression profiling biomarkers are associated with esophageal cancer detection, diagnosis, treatment, and prognosis (32). Thus, further investigations of the correlation between the above-mentioned cancer biomarkers and MRI biomarkers are warranted.

In conclusion, our observations demonstrate that DCE-MRI parameters have the potential to assess and predict treatment response to CRT. Particularly, pre-CRT K^{trans} was valuable in predicting treatment response. Moreover, marked reductions in K^{trans} and K_{ep} values were associated with good CRT response. Finally, in ROC analysis of diagnostic performance, $r\Delta K^{trans}$, the ratio of change in K^{trans} value, showed substantial advantage for assessing treatment response to CRT.

Conflict of interest disclosure

The authors declared no conflicts of interest.

References

1. Ferlay J, Shin HR, Bray F, et al. Estimates of worldwide burden of cancer in 2008: GLOBOCAN 2008. Int J Cancer 2010; 127:2893–2917. [CrossRef]
2. Pennathur A, Gibson MK, Jobe BA, et al. Oesophageal carcinoma. Lancet 2013; 381:400–412. [CrossRef]
3. Liu S, Zhen FX, Sun NN, et al. Apparent diffusion coefficient values detected by diffusion-weighted imaging in the prognosis of patients with locally advanced esophageal squamous cell carcinoma receiving chemoradiation. Onco Targets Ther 2016; 9:5791–5796. [CrossRef]
4. Heethuis SE, Rossum PSN, Lips IM, et al. Dynamic contrast-enhanced MRI for treatment response assessment in patients with oesophageal cancer receiving neoadjuvant chemoradiotherapy. Radiother Oncol 2016; 120:128–135. [CrossRef]
5. Rossum PSN, Lier ALHMW, Vulpen M, et al. Diffusion-weighted magnetic resonance imaging for the prediction of pathologic response to neoadjuvant chemoradiotherapy in esophageal cancer. Radiother Oncol 2015; 115:163–170. [CrossRef]
6. Imanishi S, Shuto K, Aoyagi T, et al. Diffusion-weighted magnetic resonance imaging for predicting and detecting the early response to chemoradiotherapy of advanced esophageal squamous cell carcinoma. Dig Surg 2013; 30:240–248. [CrossRef]
7. Wang CH, Yin FF, Horton J, et al. Review of treatment assessment using DCE-MRI in breast cancer radiation therapy. World J Methodol 2014; 4:46–58. [CrossRef]
8. Huang W, Beckett BR, Tudorica A, et al. Evaluation of soft tissue sarcoma response to preoperative chemoradiotherapy using dynamic contrast-enhanced magnetic resonance imaging. Tomography 2016; 2:308–316. [CrossRef]
9. Kim JH, Kim CK, Park BK, et al. Dynamic contrast-enhanced 3-T MR imaging in cervical cancer before and after concurrent chemoradiotherapy. Eur Radiol 2012; 22:2533–2599. [CrossRef]
10. Chikui T, Kitamoto E, Kawano S, et al. Pharmacokinetic analysis based on dynamic contrast-enhanced MRI for evaluating tumor response to preoperative therapy for oral cancer. J Magn Reson Imaging 2012; 36:589–597. [CrossRef]
11. Xu XQ, Choi YJ, Sung YS, et al. Intravoxel incoherent motion MR imaging in the head and neck: correlation with dynamic contrast-enhanced MR imaging and diffusion-weighted imaging. Korean J Radiol 2016; 17:641–649. [CrossRef]
12. Tong T, Sun YQ, Gollub MJ, et al. Dynamic contrast-enhanced MRI: use in predicting pathological complete response to neoadjuvant chemoradiation in locally advanced rectal cancer. J Magn Reson Imaging 2015; 42:673–680. [CrossRef]
13. Lerant G, Sarkozy P, Takacsi-Nagy Z, et al. Dynamic contrast-enhanced MRI parameters as biomarkers in assessing head and neck lesions after chemoradiotherapy using a wide-bore 3 Tesla scanner. Pathol Oncol Res 2015; 21:1091–1099. [CrossRef]
14. Lei J, Han Q, Zhu SC, et al. Assessment of esophageal carcinoma undergoing concurrent chemoradiotherapy with quantitative dynamic contrast-enhanced magnetic resonance imaging. Oncol Lett 2015; 10:3607–3612. [CrossRef]
15. Oberholzer K, Pohlmann A, Schreiber W, et al. Assessment of tumor microcirculation with dynamic contrast-enhanced MRI in patients with esophageal cancer: initial experience. J Magn Reson Imaging 2008; 27:1296–1301. [CrossRef]
16. Chang EY, Li X, Jerosch-Herold M, et al. The evaluation of esophageal adenocarcinoma using dynamic contrast-enhanced magnetic resonance imaging. J Gastrointest Surg 2008; 12:166–175. [CrossRef]
17. Eisenhauer EA, Therasse P, Bogaerts J, et al. New response evaluation criteria in solid tumors: revised RECIST guideline (version 1.1). Eur J Cancer 2009; 45:228–247. [CrossRef]
18. Intven M, Reerink O, Philippens MEP. Dynamic contrast enhanced MR imaging for rectal cancer response assessment after neo-adjuvant chemoradiation. J Magn Reson Imaging 2015; 41:1646–1653. [CrossRef]
19. Cooper RA, Carrington BM, Loncaster JA, et al. Tumor oxygenation levels correlate with dynamic contrast-enhanced magnetic resonance imaging parameters in carcinoma of the cervix. Radiother Oncol 2000; 57:53–59. [CrossRef]
20. King AD, Thoeny HC. Functional MRI for the prediction of treatment response in head and neck squamous cell carcinoma: potential and limitations. Cancer Imaging 2016; 16:23. [CrossRef]
21. Lee HY, Kim N, Goo JM, et al. Perfusion parameters as potential imaging biomarkers for the early prediction of radiotherapy response in a rat tumor model. Diagn Interv Radiol 2016; 22:231–240. [CrossRef]
22. Kim SH, Lee JM, Gupta SN, et al. Dynamic contrast-enhanced MRI to evaluate the therapeutic response to neoadjuvant chemoradiation therapy in locally advanced rectal cancer. J Magn Reson Imaging 2014; 40:730–737. [CrossRef]
23. de Lussanet QG, Backes WH, Griffioen AW, et al. Dynamic contrast-enhanced magnetic resonance imaging of radiation therapy-induced microcirculation changes in rectal cancer. Int J Radiat Oncol Biol Phys 2005; 63:13509–1315. [CrossRef]
24. Zahra MA, Hollingsworth KG, Sala E, et al. Dynamic contrast-enhanced MRI as a predictor of tumor response to radiotherapy. Lancet Oncol 2007; 8:63–74. [CrossRef]
25. Lim JS, Kim D, Baek SE, et al. Perfusion MRI for the prediction of treatment response after preoperative chemoradiotherapy in locally advanced rectal cancer. Eur Radiol 2012; 22:1693–1700. [CrossRef]
26. Bollschweiler E, Hölscher AH, Schmidt M, et al. Neoadjuvant treatment for advanced esophageal cancer: response assessment before surgery and how to predict response to chemoradiation before starting treatment. Chin J Cancer Res 2015; 27:221–230.

27. Hou J, Yu XP, Hu Y, et al. Value of intravoxel incoherent motion and dynamic contrast-enhanced MRI for predicting the early and short-term responses to chemoradiotherapy in nasopharyngeal carcinoma. Medicine (Baltimore) 2016; 95:e4320. [CrossRef]
28. Ng SH, Lin CY, Chan SC, et al. Dynamic contrast-enhanced MR imaging predicts local control in oropharyngeal or hypopharyngeal squamous cell carcinoma treated with chemoradiotherapy. PLoS One 2013; 8:e72230. [CrossRef]
29. Guo J, Reddick WE, Glass JO, et al. Dynamic contrast-enhanced magnetic resonance imaging as a prognostic factor in predicting event-free and overall survival in pediatric patients with osteosarcoma. Cancer 2012; 118:3776–3785. [CrossRef]
30. Chawla S, Kim S, Dougherty L, et al. Pretreatment diffusion-weighted and dynamic contrast-enhanced MRI for prediction of local treatment response in squamous cell carcinomas of the head and neck. AJR Am J Roentgenol 2013; 200:35–43. [CrossRef]
31. Lin M, Tian MM, Zhang WP, et al. Predictive values of diffusion-weighted imaging and perfusion-weighted imaging in evaluating the efficacy of transcatheter arterial chemoembolization for hepatocellular carcinoma. Onco Targets Ther 2016; 9:7029–7037. [CrossRef]
32. Tan C, Qian X, Guan ZF, et al. Potential biomarkers for esophageal cancer. Springerplus 2016; 5:467. [CrossRef]